

Organic & Biomolecular Chemistry

Accepted Manuscript



This article can be cited before page numbers have been issued, to do this please use: J. Haas, M. Häckh, V. Justus, M. Muller and S. Lüdeke, *Org. Biomol. Chem.*, 2017, DOI: 10.1039/C7OB02666H.



This is an Accepted Manuscript, which has been through the Royal Society of Chemistry peer review process and has been accepted for publication.

Accepted Manuscripts are published online shortly after acceptance, before technical editing, formatting and proof reading. Using this free service, authors can make their results available to the community, in citable form, before we publish the edited article. We will replace this Accepted Manuscript with the edited and formatted Advance Article as soon as it is available.

You can find more information about Accepted Manuscripts in the [author guidelines](#).

Please note that technical editing may introduce minor changes to the text and/or graphics, which may alter content. The journal's standard [Terms & Conditions](#) and the ethical guidelines, outlined in our [author and reviewer resource centre](#), still apply. In no event shall the Royal Society of Chemistry be held responsible for any errors or omissions in this Accepted Manuscript or any consequences arising from the use of any information it contains.



Journal Name

ARTICLE

Addition of a polyhistidine tag alters the regioselectivity of carbonyl reductase S1 from *Candida magnoliae*

Julian Haas,^a Matthias Häckh,^a Viktor Justus,^a Michael Müller^a and Steffen Lüdeke*^a

Received 00th January 20xx,
Accepted 00th January 20xx

DOI: 10.1039/x0xx00000x

www.rsc.org/

Studying enzymatic reductions of substrates with more than a single keto group is challenging, as the carbonyl reduction can create a vast array of regio- and stereoisomers. If used as reference compounds, regio- and stereopure hydroxy ketides could facilitate the characterization of reductases with unclear regio- and stereoselectivity. We have combined nonenzymatic and enzymatic reduction and oxidation steps to obtain all four regio- and stereoisomers of *tert*-butyl hydroxyoxohexanoates in high optical purity (enantiomeric ratio (er) of 99:1 for the δ -hydroxy- β -keto isomers; er of >97:3 for the β -hydroxy- δ -keto isomers). Furthermore, we have prepared seven of the eight possible regioisomers and diastereomers of γ -methylated hydroxyoxohexanoates. These 11 compounds allowed unraveling the complex stereoselectivity of β,δ -diketo ester reductions catalyzed by carbonyl reductase S1 from *Candida magnoliae* (CMCR-S1). Our analysis shows that the regio- and stereoselectivity of CMCR-S1-catalyzed reduction is highly sensitive toward modifications at the C-terminus of CMCR-S1: in addition to the expected δ -hydroxy product, the variant with a C-terminal His-tag also led to formation of β -hydroxy by-products with high optical purity.

Introduction

When a single carbonyl group of a polycarbonyl precursor is reduced, there are numerous possibilities for stereo- and/or regioisomers of the resulting alcohols. This concept is, for example, exploited in the biosynthesis of polyketides to create diversity in this class of highly complex natural products with alternating keto or chiral hydroxyl groups, the latter formed by enzymatic keto reduction.

Keto reductases are generally categorized as *R*- or *S*-selective according to the observed stereochemical outcome in a model reaction. However, studying the transformation of short-chain model substrates does not provide a complete picture of enzymatic selectivity and specificity: an enzyme may show opposite selectivity for small substrates, such as keto esters (a diketide in the context of polyketide biosynthesis), relative to longer-chain derivatives (triketides, tetraketides, etc.).³ In the latter case, the additional carbonyl groups even allow different regioselectivities. Therefore, longer-chain substrate models could help to unravel hitherto unknown specificities of an enzyme.

β,δ -Diketo esters, such as *tert*-butyl 3,5-dioxohexanoate (**1a**), are the simplest examples of triketides. A single keto reduction gives rise to four possibilities: *R*- or *S*-selective reduction at either the β - or δ -position. In *tert*-butyl 4-methyl-3,5-dioxohexanoate (**1b**), the alkylation at the γ -position doubles

the number of possible product isomers, since the alkyl side chain can be either *syn*- or *anti*-orientated with respect to the newly formed hydroxyl group. Highly stereoselective enzymatic reductions of **1a** and **1b** to the corresponding δ -hydroxy- β -keto esters **2a** and **2b**⁴⁻⁶ allow for nonenzymatic diastereoselective reduction at the β -position.⁷ Alternatively, several biocatalytic reactions lead to β,δ -dihydroxy products.⁸⁻¹¹ In contrast, precedence for exclusive direct enzymatic β -reduction of triketide-derived substrates is rare.⁴ Therefore, when trying to synthesize triketides selectively, chemists face a dilemma: i) the lack of catalysts (including enzymes) allowing a versatile and highly regio- and stereoselective synthesis of β -hydroxy- δ -keto esters; ii) the lack of enantiopure reference compounds hampering the identification and characterization of selective catalysts such as enzymes with β -reductase activity.

In this work, we solve this problem by presenting an enzyme-aided stereoselective route to triketides. We employ regio- and stereoselective oxidation catalyzed by NAD(P)⁺-dependent alcohol dehydrogenases (ADH) to obtain different stereoisomers of *tert*-butyl 3-hydroxy-5-oxohexanoate (**3a**) and *tert*-butyl 3-hydroxy-4-methyl-5-oxohexanoate (**3b**). The stereochemistry of the desired products was controlled by the choice of ADH, and the absolute configuration of the different stereoisomers was confirmed by vibrational circular dichroism (VCD). To demonstrate the value of selective triketide synthesis, we used 11 stereoisomers of **2a**, **2b**, **3a**, and **3b** as reference compounds for studying the regio- and stereoselectivity of diketide substrate reductions catalyzed by carbonyl reductase S1 from *Candida magnoliae* (CMCR-S1). While recombinant enzymes with an N-terminal His-tag (CMCR-S1^{N-His}) catalyzed δ -selective reductions, catalysis by

^a Institute of Pharmaceutical Sciences, University of Freiburg, Albertstraße 25, 79104 Freiburg, Germany. E-mail: steffen.luedeke@pharmazie.uni-freiburg.de
Electronic Supplementary Information (ESI) available: General methods, enzyme activity kinetics, protein stability assays, analytical data, spectra and chromatograms. See DOI: 10.1039/x0xx00000x

the C-terminal His-tag variant (CMCR-S1^{C-His}) delivered both δ - and β -hydroxy products, each with high stereoselectivity.

Results

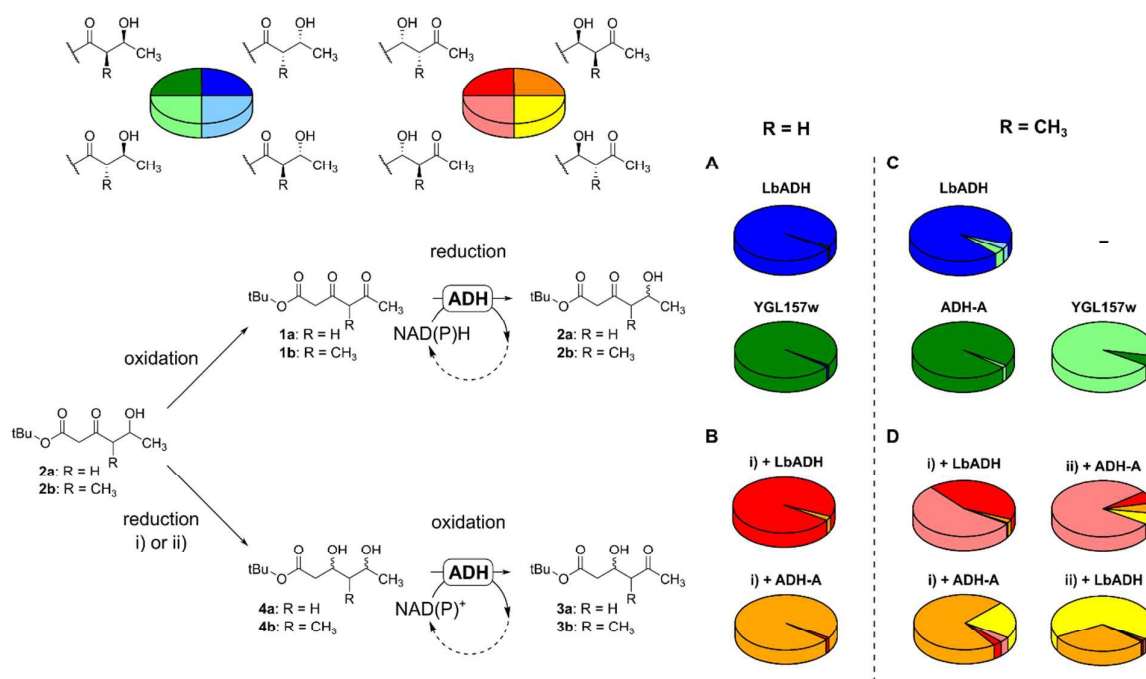
Selective route to δ,β - and β,δ -hydroxyketo esters

The two δ -hydroxy- β -keto ester enantiomers **2a** were synthesized via stereoselective keto reductions of **1a**, as described previously.^{13,14} Thus, reduction with ADH from *Lactobacillus brevis* (LbADH) gave (*R*)-**2a** and the use of ADH YGL157w from baker's yeast resulted in (*S*)-**2a** with high enantiomeric ratios (Scheme 1A). The selective synthesis of the corresponding β -hydroxy- δ -keto ester regioisomer **3a** is less trivial and usually comprises multiple steps, including enzyme catalysis.^{4,15} We aimed to develop a straightforward and versatile synthesis employing well-characterized or even commercially available ADHs. As a substrate for the crucial enzymatic oxidation step, the racemic *erythro*-diol⁵ *tert*-butyl 3,5-dihydroxyhexanoate (*erythro*-**4a**) was synthesized by diastereoselective reduction of *rac*-**2a**^{16,17} (obtained by aldol addition of acetaldehyde to *tert*-butyl acetoacetate).⁶ To obtain (*R*)-**3a** and (*S*)-**3a** from enzymatic kinetic resolution of *erythro*-**4a**, we used LbADH (the same enzyme employed for the stereoselective reduction of **1a**, see above), and ADH-A from *Rhodococcus ruber*. These enzymes were chosen according to their known opposite stereoselectivities in reduction direction. To generate a thermodynamic driving force, we combined the ADH-catalyzed oxidation reactions with a previously developed regeneration system for NAD(P)⁺,

which uses molecular oxygen from ambient air in presence of a quinone mediator as the final electron acceptor.¹² We analyzed both oxidation products by VCD spectroscopy and comparison to spectra from quantum chemical calculations, a straightforward method for the determination of the absolute configuration of chiral molecules^{18,19}. The VCD analysis confirmed the rationale of corresponding selectivities in oxidation and reduction direction and allowed the assignment of the LbADH-product to (*R*)-**3a** and the ADH-A-product to (*S*)-**3a** (Figure 1). Enantiomeric ratios (er) as given in the charts in Scheme 1B were determined by chiral-phase HPLC⁺ (Figure S5).

Stereoselective synthesis of δ,β - and β,δ -hydroxyketo- γ -methyl esters

Some ADHs show a strong preference for reducing either (*R*)- or (*S*)-**1b** in biocatalytic syntheses.^{5,6} The continuous racemization of substrate **1b** via keto-enol tautomerism allows dynamic kinetic resolution (DKR) upon ADH-catalyzed reduction of the δ -keto-group. Previously, we described the DKR of **1b** via ADH reduction of the δ -keto group, giving access to three of the four possible diastereomers of *tert*-butyl 5-hydroxy-4-methyl-3-oxohexanoate (**2b**; Scheme 1C).⁶ For the synthesis of the different stereoisomers of the β -hydroxy species **3b**, we assumed that an ADH's stereospecificity was the same in oxidation and reduction direction. According to the observations made for the DKR of **1b**,⁶ *R*-specific LbADH should preferably catalyze the oxidation of a (4*S*,5*R*)-configured substrate, while ADH-A should specifically convert the (4*R*,5*S*)-configured enantiomer. As



Scheme 1 Stereoselective synthesis of hydroxy keto esters involving ADHs for stereoselective reduction (LbADH, YGL157w, ADH-A) or stereospecific oxidation (LbADH, ADH-A). Reaction conditions: i) 1. B(OMe)Et₂ (−70 °C), 2. NaBH₄, 3. H₂O₂,^{16,17} ii) (CH₃)₄N(CH₂CO₂)₃BH (−20 °C).³³ The regio- and stereochemical composition of the resulting hydroxy keto esters are shown in pie charts, as previously introduced by Kaluzna et al.¹⁵ A) δ -Hydroxy- β -keto esters. B) β -Hydroxy- δ -keto esters. C) δ -Hydroxy- β -keto- γ -methyl esters. D) β -Hydroxy- δ -keto- γ -methyl

substrates, we synthesized racemic *erythro-4b* and *threo-4b* via diastereoselective reduction of **2b** (Scheme 1).^{16,17,33} This was the same strategy to control the configuration of the β -hydroxy group (here relative to the γ -methyl group) as applied for the non-methylated substrates.

ADH-A-catalyzed oxidation of *erythro-4b* and *threo-4b* exhibited the expected regioselectivity and stereospecificity, to afford *syn*-(3*R*,4*S*)-**3b** (24%, er = 96:4; $d_{r_{syn:anti}}$ = 75:25) and *anti*-(3*S*,4*S*)-**3b** (12%; er = 92.5:7.5; $d_{r_{syn:anti}}$ = 13:87), respectively (Scheme 1D; absolute configurations confirmed by VCD, see Figures S14 and S15). Interestingly, the LbADH-catalyzed oxidations delivered two diastereomers each for *erythro-4b* and *threo-4b* (Scheme 1D), suggesting a lower stereospecificity for the configuration of the γ -methyl group in the oxidation direction than in LbADH-catalyzed reductions. Nevertheless, as the retention times of *syn*-(3*R*,4*S*)-**3b** and *anti*-(3*S*,4*S*)-**3b** could be assigned, it was possible to deduce the elution order and determine the dr of all four diastereomers of **3b** by chiral-phase HPLC (Figure S8).

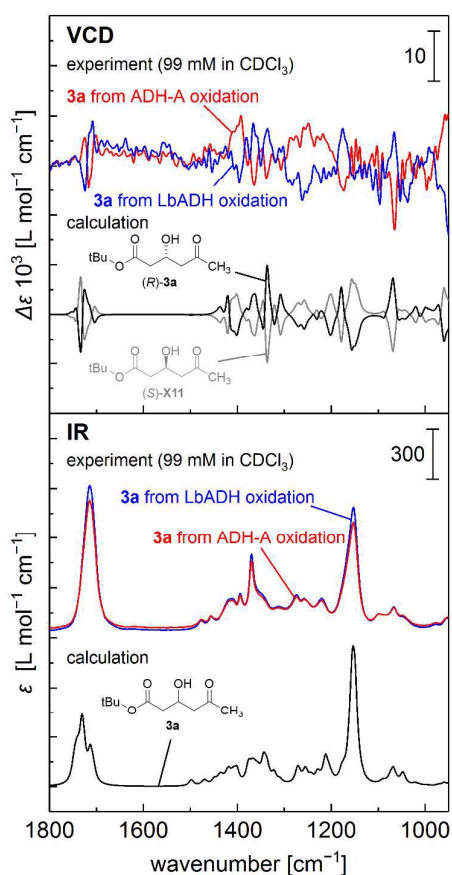


Figure 1 Experimental VCD and IR spectra of *tert*-butyl 3-hydroxy-5-oxohexanoate (**3a**) from the oxidation of *tert*-butyl *syn*-3,5-dihydroxyhexanoate (*erythro-4a*) catalyzed by ADH-A (red) and LbADH (blue) in comparison to calculated spectra for the enantiomers (*R*)-**3a** (black) and (*S*)-**3a** (gray).

Stereo- and regioselectivity of CMCR-S1-catalyzed reductions

With an array of different regio- and stereoisomers of methylated and non-methylated hydroxyketo esters of moderate to high optical purity in hand, it was possible to examine the stereoselectivity behavior of keto reductases toward triketide-derived substrates. CMCR-S1, an enzyme whose physiological substrate is unknown, was chosen as a model. Similar to other short chain dehydrogenases/reductases (SDRs) from *Candida* species,^{20,21} CMCR-S1 displays high selectivity in the reduction of carbonyl substrates, and therefore has a high potential for use as a catalyst in the synthesis of chiral building blocks.²² This potential has been demonstrated for whole cell transformations of ethyl 4-chloroacetoacetate and ethyl acetoacetate with overexpressed CMCR-S1 in *E. coli*, yielding high product concentrations.^{23,24}

The codon-optimized sequence for CMCR-S1 was cloned into the pET-19b vector (for an N-terminal His-tag) or the pET-22b(+) vector (for C-terminal His-tag) and the corresponding fusion proteins CMCR-S1^{N-His} and CMCR-S1^{C-His} were produced in *E. coli*. The His-tag was introduced to allow purification by affinity chromatography prior to enzymatic conversions, to avoid background reactions from cell lysate enzymes. To obtain isolated CMCR-S1^{wt}, the N-terminal His-tag from purified CMCR-S1^{N-His} was cleaved with enterokinase. The circular dichroism (CD) spectra of the three variants (Figure S1) indicate a high α -helix content superimposed with a β -sheet pattern^{25,26} as expected for a properly folded SDR with a Rossmann-fold motif.²⁷⁻²⁹ The three variants also had a similar thermal denaturation behavior (Figure S2), with melting temperatures of 56 °C (CMCR-S1^{wt}), 52 °C (CMCR-S1^{N-His}), and 50 °C (CMCR-S1^{C-His}). Slightly decreased thermostability after addition of a His-tag is not unusual, and has already been reported for other proteins.^{30,31} All three variants showed activity for the conversion of ethyl 4-chloroacetoacetate, albeit with a significantly lower specific activity (<1%) of CMCR-S1^{C-His} (0.8 U mg⁻¹) relative to CMCR-S1^{N-His} (109.2 U mg⁻¹). This can be explained by the C-terminus being generally closer to the active site in SDRs than the N-terminus,³² and thus possible interference with the enzyme-substrate interaction. The specific activity of CMCR-S1^{wt} (12.0 U mg⁻¹) was also lower than that of CMCR-S1^{N-His}, most probably due to a loss in activity after the enterokinase treatment. Still, the specific activity of CMCR-S1^{wt} was 15-fold higher than that of CMCR-S1^{C-His}.

The enzymatic reduction of diketo substrate **1a** catalyzed by CMCR-S1^{N-His} afforded predominantly the δ -hydroxy product **2a**. VCD analysis (Figure S11) and comparison of the HPLC chromatogram of the CMCR-S1^{N-His} reduction product with those of the reference compounds (Figure S6) allowed the assignment of the *R*-configuration (CMCR-S1^{N-His}; er = 98.5:1.5; Scheme 2A). This is consistent with the stereoselectivity previously observed for the conversion of ethyl 4-chloroacetoacetate.²² In contrast, the conversion of **1a** in the presence of CMCR-S1^{C-His} afforded two products: the regioisomers **2a** and **3a** (84:16; assigned by NMR spectroscopy,

Figure S17). The availability of reference compounds for all four possible isomeric reduction products allowed a qualitative and quantitative stereochemical analysis by chiral-phase HPLC (Figure S6). Reduction at the δ -position catalyzed by CMCR-S1^{C-His} occurred with the same selectivity as for CMCR-S1^{N-His}, yielding (*R*)-**2a** (er = 98.5:1.5). In addition, formation of the β -hydroxy product (*R*)-**3a** (16%, er = 95:5) was observed (Scheme 2A). In comparison to CMCR-S1^{N-His}, CMCR-S1^{C-His} seems to provide an alternative reaction path for β,δ -diketo ester reductions with marked stereoselectivity for reduction of diketone **1a** at the β -position. The high stereopurity of the by-product suggests that β -reduction is not a random, but rather a selective process involving the existence of a highly specific binding mode in addition to the one responsible for selective δ -reduction.

NMR spectroscopy and GC-MS analysis revealed that CMCR-S1^{N-His} reduces the methylated diketone **1b** solely at the δ -position. HPLC analysis (Figure S9) and comparison to the δ -hydroxy reference compounds **2b** indicated *R*-selectivity and high diastereoselectivity for *syn*-(4*S*,5*R*)-**2b** (er = 98:2; dr_{*syn:anti*} = 85:15; Scheme 2B).

CMCR-S1^{C-His} reduction of **1b**, however, yielded two regioisomers: δ -hydroxy- β -keto ester **2b** and β -hydroxy- δ -keto ester **3b**. Compared to the reduction of **1a**, the β -hydroxy product was formed in considerably higher amounts (**2b**:**3b** = 62:38, Scheme 2). Surprisingly, HPLC analysis (Figure S9) revealed different δ -hydroxy diastereomers for the CMCR-S1^{C-His} and CMCR-S1^{N-His} reductions. The CMCR-S1^{C-His} reduction afforded predominantly *anti*-(4*S*,5*S*)-**2b**, albeit with moderate enantio- and diastereoselectivity (er = 89:11, dr_{*syn:anti*} = 21:79). The β -hydroxy product was identified as *anti*-(3*S*,4*S*)-**3b**, which was formed with high enantio- and diastereoselectivity (er = 95:5, dr_{*syn:anti*} = 9:91; Scheme 2B). These findings suggest that the additional methyl group interferes more with

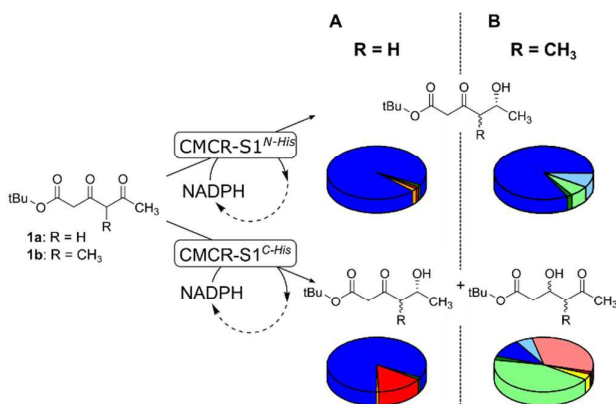
latter still occurring with high stereoselectivity and stereospecificity.

Bispecificity of CMCR-S1

According to these findings, CMCR-S1 provides two independent and highly selective reaction paths. Variation of the C-terminus, here serendipitously undertaken by the introduction of a His-tag, was sufficient to reveal the previously unknown β -reduction pathway.

Two hypotheses can be advanced to explain the observed bispecific behavior of CMCR-S1^{C-His}: 1) The C-terminal His-tag invokes the formation of an additional binding mode for substrates **1a** and **1b**, which coincidentally leads to high stereoselectivity and stereospecificity for keto reductions at the β -position. In this regard, it is known that the C-terminal loop of SDRs is involved in recognition, binding and positioning of the substrate.³⁴⁻⁴⁰ 2) More likely, binding modes for δ -specificity and for β -specificity are already present in the wild-type enzyme. Here, the δ -reducing binding mode is strongly favored, thereby rendering contributions from the β -specific binding kinetically negligible. However, in CMCR-S1^{C-His}, the hexa-His extension of the C-terminus somehow reduces substrate affinity to the δ -reducing binding mode and thus the contribution from the β -reducing binding mode becomes more important (Figure 2). The considerably higher Michaelis constant (determined for ethyl 4-chloroacetoacetate; Figure S3) for CMCR-S1^{C-His} (K_m = 19.55 mM) than for CMCR-S1^{wt} (K_m = 6.7 mM) and CMCR-S1^{N-His} (K_m = 9.10 mM) suggests that substrate binding is hindered in presence of a C-terminal His-tag. However, the substrate used for K_m determination only contains a single keto group and the K_m value alone cannot provide information about the competition of two binding modes with different substrate affinity.

To substantiate the competing binding modes-hypothesis experimentally, we tested the regioisomeric product composition after CMCR-S1-catalyzed conversion (pH 7.0, 24 hours) of diketone **1a** at different substrate/enzyme ratios (Figure 2). At high enzyme concentrations (low substrate/enzyme ratio), the influence of binding affinities is crucial and the substrate will preferably bind in a mode that leads to a more stable substrate–enzyme complex. In the model depicted in Figure 2A, this is the binding mode responsible for δ -reduction and, accordingly, at high enzyme concentrations there will be a large excess of the δ -reduced regioisomer. Indeed, for the CMCR-S1^{N-His}-catalyzed reduction at an enzyme concentration of 0.89 mg·mL⁻¹, virtually full conversion of **1a** into the δ -hydroxy product **2a** was observed (δ : β = 99:1, Figure 2A). With a large substrate excess at low enzyme concentrations (high substrate/enzyme ratio), binding affinities are less important. Correspondingly, the regioselectivity of CMCR-S1^{N-His}-catalyzed reduction was decreased at enzyme concentrations of 0.09 and 0.18 mg·mL⁻¹, giving rise to detectable amounts of the β -hydroxy regioisomer **3a**, albeit at lower overall conversions after 24 hours. These observations are consistent with the hypothesis that both binding modes are intrinsically present in the enzyme.



Scheme 2 Regio- and stereochemical outcome of the reduction of β,δ -diketo esters catalyzed by CMCR-S1^{N-His} or CMCR-S1^{C-His}, shown in pie charts according to the structures given in Scheme 1. A) Reduction of **1a**. B) Reduction of **1b**.

substrate specificity for δ -reduction than for β -reduction, the

At low enzyme concentrations, the overall conversion of **1a** with CMCR-S1^{C-His} catalysis is lower than with CMCR-S1^{N-His} (Figure 2B). This was expected from the low specific activity and the high K_m value for CMCR-S1^{C-His} (see above). However, with this variant, the proportion of the β -hydroxy product **3a** is considerably higher (up to $\delta:\beta = 62:38$ at 0.09 mg·mL⁻¹ enzyme). Similar to CMCR-S1^{N-His}, an increase in enzyme concentration favors the formation of **2a**; however, at high enzyme concentrations, the $\delta:\beta$ -ratio converges to $\sim 80:20$. These findings indicate a lower preference for δ -specific binding in CMCR-S1^{C-His} (Figure 2B).

Conclusions

We have presented the highly versatile, regio- and stereoselective synthesis of 11 of the 12 possible chiral *tert*-butyl hydroxyoxohexanoates with and without methylation at the γ -position. These esters were used as reference compounds to characterize the selectivity of the enzymatic keto reduction of substrates with multiple carbonyl groups. Thus, the well-known enzyme CMCR-S1 delivers two regioisomeric hydroxy keto esters upon reduction of the artificial triketides **1a** and **1b**. Particularly, the highly stereoselective and stereospecific reduction at the β -position was unexpected. This β -reduction seems to be an intrinsic property of CMCR-S1; until now, this property had remained undetected, which underlines the necessity to include longer-chain substrates in enzyme characterization studies. We have confirmed a role of the C-terminus in SDRs in substrate recognition.³⁴⁻⁴⁰ In the case of CMCR-S1^{C-His}, the His-tag at the C-terminus results in an unexpected shift from one highly specific binding mode to the other and a substrate-dependence of the stereoselectivity that was not observed in the absence of the His-tag. These findings suggest that reductases might carry multiple specificities and selectivities, in addition to the dominating effect that is generally regarded as the physiological activity. The hidden activities might be rendered more dominant by marginal modifications, such as elongation of the C-terminus. Possibly, nature utilizes hidden activities in enzymes as an optional 'add-on' feature to generate a high diversity of natural products from a minimal mutational effort.

Experimental

Molecular cloning, protein production and purification

All restriction, PCR and cloning steps were performed according to standard procedures.⁴¹ The synthetic codon-optimized genes for CMCR-S1 and ADH-A were obtained from GenScript (Piscataway, USA) and Thermo Fisher Scientific (Waltham, USA), respectively. The amplified CMCR-S1 gene (see ESI for PCR primers) was cloned into the vectors pET-19b (encodes for an N-terminal His-tag) and pET-22b(+) (C-terminal His-tag) (both Merck KGaA, Darmstadt, Germany) using the NdeI (5') and XhoI (3') restriction sites. The synthetic ADH-A gene was delivered with a 15 base pair overlap on each side,

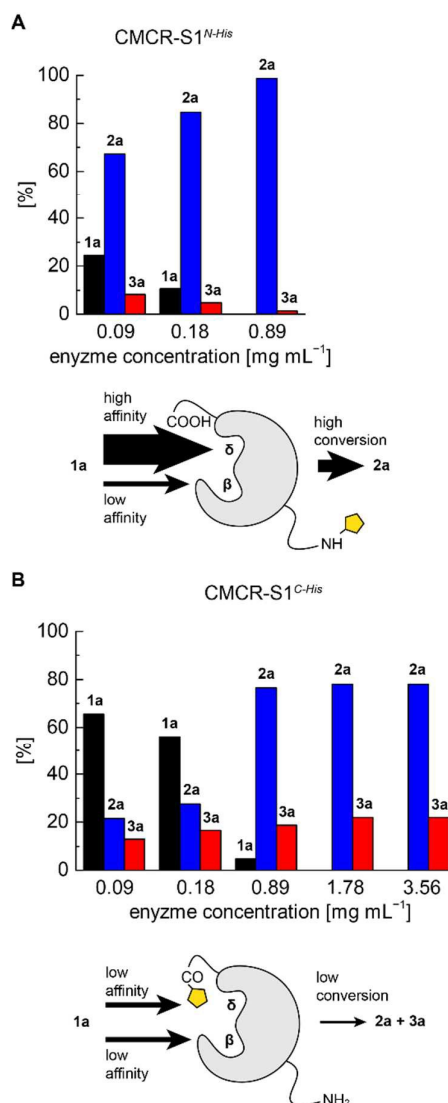


Figure 2 Substrate/product composition from the reduction of *tert*-butyl 3,5-dioxohexanoate (**1a**) catalyzed by CMCR-S1^{N-His} (A) and CMCR-S1^{C-His} (B) at different enzyme concentrations. The cartoons illustrate the two scenarios as a model of two competing binding modes for δ -reduction and β -reduction. In CMCR-S1^{N-His}, δ -specific binding is largely dominant. In CMCR-S1^{C-His}, the modification at the C-terminus interferes with binding in the δ -mode, thereby reducing the overall turnover, but increases the contribution of β -mode binding to the overall outcome.

complementary to the ends of linearized pET-19b vector (see ESI), which allowed cloning of the amplified gene with the In-Fusion HD Cloning Plus kit (Takara, Kyoto, Japan). From the resulting vector, the gene was cloned into pET-22b(+) using the restriction sites NdeI (5') and BamHI (3'), resulting in an expression vector that does not encode for a His-tag. The vectors were transformed in competent *E. coli* TG1 cells for amplification and in competent *E. coli* BL21(DE3) cells for heterologous overexpression (both Agilent Technologies, Santa Clara, USA).

After inoculation with 5 mL of an overnight starter culture (100 $\mu\text{g}\cdot\text{mL}^{-1}$ ampicillin-containing LB-Lennox medium; Carl Roth GmbH, Karlsruhe, Germany), the *ADH-A* gene was expressed in 500 mL of Studier's auto induction medium⁴² (ZY-medium, salt solution M and solution 5052 as carbon source) containing 100 $\mu\text{g}\cdot\text{mL}^{-1}$ ampicillin and incubated at 24 °C and 160 rpm for 24 h. For CMCR-S1^{N-His} and CMCR-S1^{C-His}, 400 mL of ampicillin-containing (100 $\mu\text{g}\cdot\text{mL}^{-1}$) LB-Lennox medium was inoculated with 4 mL of an overnight starter culture. After the culture was grown to an optical density of 0.6 ($\lambda = 600$ nm), the expression was induced by addition of IPTG (0.8 mM) and the protein was produced during incubation at 37 °C and 160 rpm for 4 h. LbADH, YGL157w and NfsB were expressed and produced in *E. coli* as described elsewhere.^{6,12,43} *E. coli* cells were harvested by centrifugation (15000g, 4 °C, 15 min). After resuspension in KPi buffer (50 mM, pH 7.5; 0.5 mL per 100 mL culture), the cells were disrupted by sonication (6 \times 15 s with 10 s intermission; Branson Sonifier II W-250; Heinemann, Schwäbisch Gmünd, Germany). Cell debris was removed by centrifugation (12000g, 4 °C, 45 min). CMCR-S1^{N-His} and CMCR-S1^{C-His} were purified by affinity chromatography on Ni-NTA agarose (Qiagen, Hilden, Germany). Nonspecifically bound proteins were washed off with KPi buffer (50 mM, pH 7.5) containing 50 mM imidazole (CMCR-S1^{N-His}) or 25 mM imidazole (CMCR-S1^{C-His}). CMCR-S1^{N-His} and CMCR-S1^{C-His} were eluted with KPi buffer (50 mM, pH 7.5) containing 500 mM or 250 mM imidazole, respectively. The volume of the elution fractions was reduced to 5 mL by ultrafiltration (4500g; Vivaspin 20 centrifugal concentrator, 10000 MWCO PES; Sartorius Stedim Biotech GmbH, Göttingen, Germany) and desalted by size-exclusion chromatography (PD-10 Desalting Columns; GE Healthcare Bio-sciences AB, Uppsala, Sweden). Purified CMCR-S1^{N-His} and CMCR-S1^{C-His} were stored at 4 °C. To obtain CMCR-S1^{wt}, the His-tag was cleaved from purified CMCR-S1^{N-His} with enterokinase (New England Biolabs GmbH, Frankfurt, Germany) according to the manufacturer's recommendations. NfsB was purified as described previously prior to use.¹² LbADH and YGL157w were used as crude extracts. ADH-A was used as a glycerol-containing crude extract (20% v/v) to allow storage at -20 °C. The activity of the produced enzymes was determined photometrically as a function of decrease or increase in concentration of the cofactor NAD(P)H (for details, see ESI).

Organic syntheses

tert-Butyl 5-hydroxy-3-oxohexanoate (**2a**) and *tert*-butyl 5-hydroxy-4-methyl-3-oxohexanoate (**2b**) were synthesized by the aldol addition of acetaldehyde to the respective β -keto ester, as described by Lüdeke et al.⁶ The NMR data (ESI) are consistent with the literature.^{6,14} *tert*-Butyl 3,5-dioxohexanoate (**1a**) was obtained via Jones oxidation⁴⁴ of **2a** (1010 mg, 5 mmol), as described by Bariotaki et al.,⁴ and purified by automated flash column chromatography (Isolera Prime, SNAP KP-Sil cartridge: 50 g, solvent gradient: cyclohexane:ethyl acetate from 98:2 to 78:22, flow rate: 50 mL \cdot min⁻¹) yielding 589 mg (58%) of **1a**. *tert*-Butyl 4-methyl-3,5-dioxohexanoate (**1b**) was synthesized by acylation of *tert*-

butyl 3-oxopentanoate with *N*-methoxy-*N*-methylacetamide.^{6,45} Racemic *tert*-butyl *erythro*-3,5-dihydroxyhexanoate (*erythro*-**4a**, 55%, $\text{dr}_{\text{erythro:threo}} = 40:1$) was obtained by diastereoselective reduction of **2a** (1740 mg, 8.6 mmol) as described by Thottathil et al.¹⁷ Accordingly, *tert*-butyl *erythro*-3,5-dihydroxy-4-methylhexanoate (*erythro*-**4b**; 67%; $\text{dr}_{\text{erythro:threo}} = 39:1$) was synthesized from **2b** (2500 mg, 11.6 mmol). Both diols were purified by flash column chromatography on silica gel (*erythro*-**4a**: cyclohexane:ethyl acetate 1:1, *erythro*-**4b**: cyclohexane:ethyl acetate 2:1; see ESI for analytical data). For the synthesis of *tert*-butyl *threo*-3,5-dihydroxy-4-methylhexanoate (*threo*-**4b**) from **2b** (230 mg, 1 mmol), the *anti*-selective reduction method of Evans and Chapman³³ provided 206 mg (86%) of *threo*-**4b** ($\text{dr}_{\text{erythro:threo}} = 1:58$, GC-MS; see ESI for analytical data).

Enzymatic reductions

Substrates according to Scheme 1 (1 equiv), glucose (5 equiv) and 0.05 equiv of cofactor (NAD⁺ for LbADH, YGL157w, CMCR-S1^{N-His} and CMCR-S1^{C-His}; NAD⁺ for ADH-A) were dissolved in KPi buffer (50 mM, pH 7.0; 50 mL buffer per mmol substrate). *E. coli* lysate containing the respective ADH was added to a final activity of 20 (LbADH) or 1.0 U \cdot mL⁻¹ (YGL157w and ADH-A, see ESI for details on enzyme activity determination). CMCR-S1^{N-His} (1.1 U \cdot mL⁻¹) and CMCR-S1^{C-His} (0.03 U \cdot mL⁻¹) were used as purified enzymes. For LbADH-catalyzed reductions, the mixture additionally contained 1 mM MgCl₂. Glucose dehydrogenase (GDH; 200 U per mmol substrate) for regeneration of NAD(P)H was added to start the reaction. Mixtures were stirred smoothly at room temperature and sampled periodically for TLC monitoring. Reactions were quenched by addition of NaCl (0.25 g per mL solvent), after 24 h or when the monitoring indicated complete conversion. The mixture was extracted with ethyl acetate. Precipitated proteins were removed from the organic phase by filtration over Celite 535. The organic extracts were dried over Na₂SO₄ and concentrated *in vacuo*. If necessary, the crude product was purified by flash column chromatography. Conversion yields were determined by ¹H NMR spectroscopy. Diastereomeric ratios (dr) correspond either to the ratio of ¹H NMR integrals or to peak areas (AUC) in the GC-MS chromatograms. Enantiomeric ratios (er) were determined by chiral HPLC (see ESI). The absolute configuration of optically pure products was confirmed by VCD. Conversions at various CMCR-S1^{N-His} or CMCR-S1^{C-His} concentrations (Figure 2) were carried out on an analytical scale (4 mg \pm 0.02 mmol of **1a**, 6 U GDH, 1 mL) and were quantified by GC-MS analysis directly after ethyl acetate extraction.

The analytical data for (*R*)-**2a** from LbADH-catalyzed reduction of **1a** (>99% conversion, er = 99:1) or from reductions catalyzed by CMCR-S1^{N-His} (89%, er = 98.5:1.5) or CMCR-S1^{C-His} (84%, er = 98.5:1.5), and for (*S*)-**2a** (YGL157w; 84%, er = 99:1) were consistent with those for **2a** synthesized by aldol addition of acetaldehyde to *tert*-butyl acetoacetate (see above). The identity of the methylated species *syn*-(4*S*,5*R*)-**2b** from LbADH-catalyzed (>99%, er >99:1, $\text{dr}_{\text{syn:anti}} = 93:7$) or CMCR-S1^{N-His}-catalyzed reduction of **1b** (61%, er = 98:2, $\text{dr}_{\text{syn:anti}} = 85:15$), of

syn-(4*R*,5*S*)-**2b** from ADH-A-catalyzed reduction of **1b** (>99%, er >99:1, $dr_{syn:anti} = 98:2$), and of *anti*-(4*S*,5*S*)-**2b** from YGL157w-catalyzed (70%, er >99:1, $dr_{syn:anti} = 6:94$) or CMCR-S1^{C-His}-catalyzed reduction of **1b** (62%, er = 89:11, $dr_{syn:anti} = 21:79$) was confirmed by comparison to the analytical data for *syn/anti*-**2b** obtained by aldol addition of acetaldehyde to *tert*-butyl 3-oxopentanoate (see above). The β -hydroxy- δ -keto esters (*R*)-**3a**, (16%, er = 95:5), and *anti*-(3*S*,4*S*)-**3b** (38%, er = 95:5, $dr_{syn:anti} = 9:91$), obtained as byproducts from CMCR-S1^{C-His} reduction of **1a** and **1b**, respectively, were not separable from the corresponding δ -hydroxy- β -keto esters by flash column chromatography. Therefore, and to avoid adulteration of the regio- and stereochemical composition from purification, their identity and the isomeric ratios were determined chromatographically for the crude reduction products through comparison with the reference compounds from enzymatic oxidations (see below).

Enzymatic oxidations

Substrates according to Scheme 1 (1 equiv), 0.05 equiv of the oxidized cofactor (NADP⁺ for LbADH, NAD⁺ for ADH-A) and lawsone (0.05 equiv) were dissolved in Tris HCl buffer (50 mM, pH 8.0; 50 mL buffer per mmol substrate). *E. coli* lysate containing either LbADH or ADH-A was added to a final activity of 3 U·mL⁻¹ (see ESI for details on enzyme activity determination). For LbADH-catalyzed oxidations, the mixture additionally contained 1 mM MgCl₂. Purified NfsB (2000 U per mmol substrate) was added for cofactor regeneration. Reactions were quenched by addition of NaCl (0.25 g per mL solvent), after stirring at room temperature for 20 h. The mixture was extracted with ethyl acetate, and precipitated enzymes were removed from the organic phase by filtration over Celite 535. The organic extracts were washed with aqueous NaOH solution (0.01 M) and deionized water, dried over Na₂SO₄ and concentrated *in vacuo*. The crude products were purified by automated flash column chromatography (Isolera Prime, SNAP KP-Sil cartridge: 25 g, solvent gradient: cyclohexane:ethyl acetate from 88:12 to 0:100, flow rate: 25 mL·min⁻¹). The *dr* was calculated from ¹H NMR integrals or the AUCs in GC-MS chromatograms. The *er* was obtained from the AUCs in chiral HPLC chromatograms.

Oxidation of *erythro*-**4a** (204 mg, 1 mmol) catalyzed by LbADH afforded 72 mg of *tert*-butyl (*R*)-3-hydroxy-5-oxohexanoate ((*R*)-**3a**) after purification (36%, er = 97.5:2.5), while ADH-A catalysis yielded 74 mg of purified *tert*-butyl (*S*)-3-hydroxy-5-oxohexanoate ((*S*)-**3a**, 37%, er = 98.5:1.5). ADH-A oxidation of *erythro*-**4b** (218 mg, 1 mmol) led to 52 mg (24%) of purified *tert*-butyl *syn*-(3*R*,4*S*)-3-hydroxy-4-methyl-5-oxohexanoate (*syn*-(3*R*,4*S*)-**3b**, er = 96:4, $dr_{syn:anti} = 75:25$), while ADH-A oxidation of *threo*-**4b** gave *tert*-butyl *anti*-(3*S*,4*S*)-3-hydroxy-4-methyl-5-oxohexanoate (*anti*-(3*S*,4*S*)-**3b**, 26 mg, 12%, er = 92.5:7.5, $dr_{syn:anti} = 13:87$). LbADH-catalyzed oxidations were not stereospecific with respect to the γ -methyl group. Thus, oxidation of *erythro*-**4b** (218 mg, 1 mmol) and purification afforded 77 mg (36%) of a diastereomeric mixture of *tert*-butyl *syn/anti*-(3*S*,4*R*/*S*)-3-hydroxy-4-methyl-5-oxohexanoate (*syn/anti*-(3*S*,4*R*/*S*)-**3b**, $dr_{syn:anti} = 45:55$), while

oxidation of *threo*-**4b** gave 66 mg (31%) of a mixture of *tert*-butyl *syn/anti*-(3*R*,4*R*/*S*)-3-hydroxy-4-methyl-5-oxohexanoate (*syn/anti*-(3*R*,4*R*/*S*)-**3b**, $dr_{syn:anti} = 33:67$). The analytical data for the oxidation products are given in the ESI.

VCD analysis

For the measurement of experimental IR and VCD spectra, samples were dissolved in anhydrous CDCl₃ and placed in a rotatable BaF₂ cell (path length: 110 μ m). The measured spectra represent the average of 12 h measurements at different angles from 0° to 360° in increments of 7.5°. All spectra were background-corrected for a CDCl₃ spectrum. The concentrations of the samples are specified on the individual spectra. To facilitate the assignment of its configuration, (4*S*,5*S*)-**2b** was transformed into the six-membered lactone *trans*-(5*S*,6*S*)-5,6-dimethyldihydro-2*H*-pyran-2,4(3*H*)-dione, as described by Tabuchi et al.,⁴⁶ thereby reducing conformational freedom and increasing the signal intensity in the VCD spectrum.

For the calculation of theoretical IR and VCD spectra, conformer geometries of (*R*)-**2a**, (*R*)-**3a**, (4*R*,5*S*)-**2b**, (3*S*,4*S*)-**3b**, (3*R*,4*S*)-**3b** and *trans*-(5*S*,6*S*)-5,6-dimethyldihydro-2*H*-pyran-2,4(3*H*)-dione were generated with the MMFF-based conformer search algorithm in Spartan 08 (Wavefunction, Irvine, USA). Geometry optimizations and calculations of relative energies, IR, and VCD frequencies were performed at the DFT level in Gaussian 09⁴⁷ (in the case of **2a** and **3a** with B3LYP/6-311++G(d,p); in the case of **2b**, **3b** and **11** with B3LYP/6-31+G(d,p) and a PCM solvent model for chloroform⁴⁸). The predicted frequencies were scaled by 0.981 for B3LYP/6-311++G(d,p) and 0.983 for B3LYP/6-31+G(d,p) (scaling factors determined with VCDspecTech⁴⁹). The shown spectra represent Boltzmann-weighted averages of the conformer spectra with Lorentzian line shapes (6 cm⁻¹ bandwidth) around calculated intensities.

Acknowledgements

We thank Dr. Kay Greenfield for help in improving the manuscript. Financial support of this work by the DFG (IRTG 1038, RTG 1976) is gratefully acknowledged. This research was supported in part by the bwHPC initiative and the bwHPC-C5 project provided through associated computing services of the JUSTUS HPC facility at the University of Ulm.

Notes and references

⁵To facilitate the distinction from the *syn/anti* configuration of hydroxyl groups relative to vicinal alkyl groups, henceforth, the relative stereochemistry of two hydroxy groups is denoted as *erythro* and *threo*.

[†] To allow UV detection and to increase the resolution of the separations, all HPLC analyses in this study were performed on benzoylated derivatives.

ARTICLE

Journal Name

‡ The reported reduction product ethyl 4-chloro-3-hydroxybutanoate is S-configured, as the chlorine atom switches the CIP priority.

- H. M. O'Hare, A. Baerga-Ortiz, B. Popovic, J. B. Spencer and P. F. Leadlay, *Chem. Biol.*, 2006, **13**, 287.
- K. Faber, *Biotransformations in Organic Chemistry*, Springer, Berlin Heidelberg, 6th edn., 2011.
- H. Zhou, Z. Z. Gao, K. Qiao, J. Wang, J. C. Vederas and Y. Tang, *Nat. Chem. Biol.*, 2012, **8**, 331.
- A. Bariotaki, D. Kalaitzakis and I. Smonou, *Org. Lett.*, 2012, **14**, 1792.
- A. G. Ji, M. Wolberg, W. Hummel, C. Wandrey and M. Müller, *Chem. Commun.*, 2001, 57.
- S. Lüdeke, M. Richter and M. Müller, *Adv. Synth. Catal.*, 2009, **351**, 253.
- M. Wolberg, W. Hummel and M. Müller, *Chem. Eur. J.*, 2001, **7**, 4562.
- R. N. Patel, A. Banerjee, C. G. McNamee, D. Brzozowski, R. L. Hanson and L. J. Szarka, *Enzyme Microb. Technol.*, 1993, **15**, 1014.
- M. Müller, M. Wolberg, W. Hummel and C. Wandrey, *Germany Pat.*, DE19937825 A1, 1999.
- A. Liljeblad, A. Kallinen and L. T. Kanerva, *Curr. Org. Synth.*, 2009, **6**, 362.
- X. Luo, Y. J. Wang, W. Shen and Y. G. Zheng, *J. Biotechnol.*, 2016, **224**, 20.
- J. Haas, M. A. Schätzle, S. M. Husain, J. Schulz-Fincke, M. Jung, W. Hummel, M. Müller and S. Lüdeke, *Chem. Commun.*, 2016, **52**, 5198.
- W. A. Kaluzna, T. Matsuda, A. K. Sewell and J. D. Stewart, *J. Am. Chem. Soc.*, 2004, **126**, 12827.
- M. Wolberg, W. Hummel, C. Wandrey and M. Müller, *Angew. Chem. Int. Ed.*, 2000, **39**, 4306.
- S. Tartaglia, S. Fogal, R. Motterle, C. Ferrari, M. Pontini, R. Aureli and O. De Lucchi, *Eur. J. Org. Chem.*, 2016, 3162.
- K. M. Chen, G. E. Hardtmann, K. Prasad, O. Repic and M. J. Shapiro, *Tetrahedron Lett.*, 1987, **28**, 155.
- J. K. Thottathil, Y. Pendri, W.-S. Li and D. R. Kronenthal, *US Pat.*, US 5 278 313, 1994.
- T. B. Freedman, X. L. Cao, R. K. Dukor and L. A. Nafie, *Chirality*, 2003, **15**, 743.
- P. J. Stephens, F. J. Devlin and J.-J. Pan, *Chirality*, 2008, **20**, 643.
- N. Aggarwal, P. K. Mandal, N. Gautham and A. Chadha, *Acta Crystallogr. F*, 2013, **69**, 313.
- S. Sudhakara and A. Chadha, *Org. Biomol. Chem.*, 2017, **15**, 4165.
- D. M. Zhu, Y. Yang and L. Hua, *J. Org. Chem.*, 2006, **71**, 4202.
- N. Kizaki, Y. Yasohara, J. Hasegawa, M. Wada, M. Kataoka and S. Shimizu, *Appl. Microbiol. Biotechnol.*, 2001, **55**, 590.
- Y. Yasohara, N. Kizaki, J. Hasegawa, M. Wada, M. Kataoka and S. Shimizu, *Tetrahedron: Asymmetry*, 2001, **12**, 1713.
- N. J. Greenfield, *Nat. Protoc.*, 2006, **1**, 2876.
- G. Holzwarth and P. Doty, *J. Am. Chem. Soc.*, 1965, **87**, 218.
- H. Jörnval, J. Hedlund, T. Bergman, U. Oppermann and B. Persson, *Biochem. Biophys. Res. Commun.*, 2010, **396**, 125.
- C. Filling, K. D. Berndt, J. Benach, S. Knapp, T. Prozorovski, E. Nordling, R. Ladenstein, H. Jörnval and U. Oppermann, *J. Biol. Chem.*, 2002, **277**, 25677.
- M. G. Rossmann, D. Moras and K. W. Olsen, *Nature*, 1974, **250**, 194.
- M. Krupka, J. Masek, L. Barkoczi, P. T. Knotigova, P. Kulich, J. Plockova, R. Lukac, E. Bartheldyova, S. Koudelka, R. Chaloupkova, M. Sebel, D. Zyka, L. Droz, R. Effenberg, M. Ledvina, A. D. Miller, J. Turanek and M. Raska, *PLoS One*, 2016, **11**, 1.
- P. Ledent, C. Duez, M. Vanhove, A. Lejeune, E. Fonze, P. Charlier, F. Rhazi-Filali, I. Thamm, G. Guillaume, B. Samyn, B. Devreese, J. Van Beeumen, J. Lamotte Brasseur and J. M. Frère, *FEBS Lett.*, 1997, **413**, 194.
- K. Kavanagh, H. Jörnval, B. Persson and U. Oppermann, *Cell. Mol. Life Sci.*, 2008, **65**, 3895.
- D. A. Evans and K. T. Chapman, *Tetrahedron Lett.*, 1986, **27**, 5939.
- M. A. Schätzle, S. Flemming, S. M. Husain, M. Richter, S. Günther and M. Müller, *Angew. Chem. Int. Ed.*, 2012, **51**, 2643.
- T. Nishioka, Y. Yasutake, Y. Nishiya and T. Tamura, *FEBS J.*, 2012, **279**, 3264.
- T. Nishioka, Y. Yasutake, Y. Nishiya, N. Tamura and T. Tamura, *Proteins*, 2009, **74**, 801.
- A. C. Freydank, W. Brandt and B. Dräger, *Proteins*, 2008, **72**, 173.
- D. I. Liao, J. E. Thompson, S. Fahnestock, B. Valent and D. B. Jordan, *Biochemistry*, 2001, **40**, 8696.
- H. P. Zhou, F. X. Yan and H. H. Tai, *Eur. J. Biochem.*, 2001, **268**, 3368.
- R. Albalat, M. Valls, J. Fibla, S. Atrian and R. González-Duarte, *Eur. J. Biochem.*, 1995, **233**, 498.
- D. W. R. J. Sambrook, *Molecular cloning: A laboratory manual*, Cold Spring Harbor, New York, 3rd edn., 2000.
- F. W. Studier, *Protein Expression Purif.*, 2005, **41**, 207.
- W. Hummel, *Adv. Biochem. Eng./Biotechnol.*, 1997, **58**, 145.
- K. Bowden, I. M. Heilbron, E. R. H. Jones and B. C. L. Weedon, *J. Chem. Soc.*, 1946, 39.
- M. Wolberg, A. G. Ji, W. Hummel and M. Müller, *Synthesis*, 2001, 937.
- H. Tabuchi, T. Hamamoto, S. Miki, T. Tejima and A. Ichihara, *J. Org. Chem.*, 1994, **59**, 4749.
- M. J. Frisch, G. W. Trucks, H. B. Schlegel, G. E. Scuseria, M. A. Robb, J. R. Cheeseman, G. Scalmani, V. Barone, B. Mennucci, G. A. Petersson, H. Nakatsuji, M. Caricato, X. Li, H. P. Hratchian, A. F. Izmaylov, J. Bloino, G. Zheng, J. L. Sonnenberg, M. Hada, M. Ehara, K. Toyota, R. Fukuda, J. Hasegawa, M. Ishida, T. Nakajima, Y. Honda, O. Kitao, H. Nakai, T. Vreven, J. A. Montgomery Jr, J. E. Peralta, F. Ogliaro, M. Bearpark, J. J. Heyd, E. Brothers, K. N. Kudin, V. N. Staroverov, R. Kobayashi, J. Normand, K. Raghavachari, A. Rendell, J. C. Burant, S. S. Iyengar, J. Tomasi, M. Cossi, N. Rega, N. J. Millam, M. Klene, J. E. Knox, J. B. Cross, V. Bakken, C. Adamo, J. Jaramillo, R. Gomperts, R. E. Stratmann, O. Yazyev, A. J. Austin, R. Cammi, C. Pomelli, J. W. Ochterski, R. L. Martin, K. Morokuma, V. G. Zakrzewski, G. A. Voth, P. Salvador, J. J. Dannenberg, S. Dapprich, A. D. Daniels, Ö. Farkas, J. B. Foresman, J. V. Ortiz, J. Cioslowski and D. J. Fox, GAUSSIAN 09 (Revision D.01), Gaussian Inc., Wallingford CT, 2009.
- S. Miertuš, E. Scrocco and J. Tomasi, *Chem. Phys.*, 1981, **55**, 117.
- CDspecTech: Computer programs for calculating similarity measures of comparison between experimental and calculated dissymmetry factors and circular intensity differentials.
<https://sites.google.com/site/cdspectech1/>, version 21.7, 2015.

Journal Name

ARTICLE

Published on 23 November 2017. Downloaded by University of Newcastle on 25/11/2017 07:55:39.

Organic & Biomolecular Chemistry Accepted Manuscript

A recombinant carbonyl reductase shows different regioselectivity with a C-terminal His-tag compared to the N-tagged enzyme toward the same triketide substrate. Highly selective synthesis of reference triketides allowed solving this conundrum.

